

## FRACTURE CONTROL OF ENGINEERING STRUCTURES – ECF 6

### THE APPLICATION OF J CONCEPT TO FATIGUE CRACK GROWTH IN LARGE SCALE YIELDING

Y. Lambert, C. Bathias\*

Fatigue crack propagation tests have been performed on compact tension specimens made of AISI 316 steel in the elastic and plastic regions.

The parameter  $\Delta J$  was chosen to characterise propagation. Results show that there is a Paris law type correlation between propagation rate and  $\Delta J$ . The exponent "n" is of the same magnitude as that proposed in the literature. An effect on propagation rate which is attributed to the R ratio has been noted. Opening at the crack tip is examined.

#### INTRODUCTION

Fatigue crack propagation in metals is generally analysed for small scale yielding conditions, i.e. loading situations leading to the development of a plastic zone at the crack tip which is small in comparison to the relevant dimensions of the structure. In contrast, the exhaustive fatigue crack propagation analysis in conjunction with the "leak before break" concept has required analysis of deep cracks where the ligament between crack tip and opposite wall can be in the plastic range.

The aim of the present study is to determine the characteristics of fatigue propagation of a crack in a material under conditions from small scale yielding to general plasticity. It appears that the most suitable approach should be based on variations of the  $\Delta J$  (J integral) during a stress cycle.

\* UNIVERSITE DE COMPIEGNE - U.A. 859 du C.N.R.S. - Groupe Mécanique

## FRACTURE CONTROL OF ENGINEERING STRUCTURES – ECF 6

The objective is:

1. To demonstrate the conservation of contained yielding with test at constant  $\Delta J$  levels and with increasing values of  $a/W$ . The effects on compact tension specimen is examined.
2. To determine the laws governing fatigue propagation in uncontained plastic situations subjected to cyclic loads.
3. To closely examine the relationship between  $\Delta J$  and CTOD.

### CRACKING PARAMETERS IN THE NON ELASTIC REGION

The idea of using  $\Delta J$  as the mechanical factor governing unconfined plastic crack propagation under cyclic loading is an extension of the use of the J integral for unconfined regions under monotonic stress. Several methods have been proposed to determine  $\Delta J$  and to compare it with empirical data. The proposed methods define  $\Delta J$  using the following factors:

- \* The strain energy density in the method developed by Dowling (1), Kaisand and Mowbray (2), Liu and Lin (3) and Radhakrishnan (4). A comparison of these models has been carried out by Rye (5).
- \* The loading envelope curve, as used by Landes and McCabe (6).
- \* The COD, chosen by Tomkins (7), Tanaka (8) and Wang Shuan (9).
- \* The area under the hysteresis curve, the most studied method.

Dowling and Begley (10) and Dowling (11) established the initial equations, which were improved by Clarkes and Landes (12). A comparison for CT specimens was published by Landes (13) and the best model was used by Vardar (14).

We have selected to use the last approach since the theoretical basis appears to be the best one and it permits direct processing of empirical data discussed below.

$\Delta J$  will therefore be expressed by the formula:

$$\Delta J = \frac{2A}{Bb} \frac{(1 + \alpha)}{(1 + \alpha^2)}$$

We will interpret the empirical crack propagation rate by the expression:

$$da/dN = C \cdot \Delta J^n \quad (1)$$

## FRACTURE CONTROL OF ENGINEERING STRUCTURES – ECF 6

From a theoretical viewpoint, this model which calculates  $\Delta J$  from the  $P-\delta$  plots may be treated as a measure of energy. The total energy may be divided into two parts: a part which is dissipated in propagating the crack and a part dissipated in irreversible deformation.

For  $\Delta J$  to intrinsically govern crack propagation, the relationship between the two components of total energy must be known.

This assumes that there is a constant relationship between the variations of  $\Delta J$  and the variations of strain energy density at all points in the stress and strain fields.

During the tests, we tried to determine whether at constant values of parameter  $\Delta J$  the propagation rate remained independent of loads imposed on the test specimens.

### EXPERIMENTAL PROCEDURE

The material studied is an AISI 316 stainless steel for which the properties are presented in table 1.

The specimen type is notched Compact Tension (CT) of two different thicknesses, 35 and 50 mm. Dimensions are given in figure 1.

Tests were performed at ambient temperature on a Mayes servo-hydraulic fatigue machine of maximum capacity 260 kN. Special grips were used to permit compressive loading. An internal thread was used to prevent discontinuous loading caused by back lash in the machine.

Two types of opening transducer were used: a COD transducer in the loading axis which measured and controlled opening, and a CTOD transducer placed on the specimen surface, which followed the propagation of the crack and could be moved along the ligament.

Two methods of control were used: one involved keeping  $\Delta J$  constant and the second was by increasing  $\Delta J$ . In both cases  $\Delta J$  was calculated from the load displacement curve. Displacement was controlled to maintain a constant  $\Delta J$  or to increase it.

Analogue digital and digital analogue converters were used to interface the test machine to an Apple II computer. The ADC was used to control the load and displacement and the DAC produced sawtooth command signals.

For each cycle the displacement is adjusted either to keep  $\Delta J$  constant or to increase it. The  $\Delta J$  value for cycle  $n$  is thus calculated from the crack length at cycle  $(n-1)$ .

## FRACTURE CONTROL OF ENGINEERING STRUCTURES – ECF 6

The problem of closure was revealed for each cycle by an inflection in the tension/compression curve. It modifies the area taken into account for the calculation of  $\Delta J$ . The problem was resolved by keying in an instruction during each cycle.

The crack length was measured by the electrical potential method. A preliminary calibration by marking crack fronts was required in order to obtain the relationship between  $\Delta V/V$  and the crack length averaged over 10 points through the thickness. Optical measurements proved unsuitable due to the presence of lateral notches.

Loading of the specimen was carried out in 3 steps:

1. Precracking to initiate the crack elasticity.
2. Cracking under displacement control to reach the threshold of excessive deformation, where the elastic deformation is equal to plastic deformation. This limit is reached after a few cycles by location on the stabilized P- $\delta$  plot of the specimens. The threshold is determined experimentally and by the EPRI equation (15).
3. Crack propagation at constant or increasing  $\Delta J$ .

### RESULTS

#### Constant $\Delta J$ tests

This type of test produces contained yielding.

The hysteresis loops characteristic of control at constant  $\Delta J$  are shown in figure 2. The inflection point corresponding to the compliance change and indicating that the fracture surfaces touch and pass into compression is clearly shown. The points obtained at constant  $\Delta J$  are plotted in figure 3. It may be noted that for a given  $\Delta J$  the propagation rate is not constant but decreases slightly during the test.

#### Increasing $\Delta J$ tests

The crack propagation curve and propagation rate as a function of the  $\Delta J$  parameter, in figure 4 shows a linear relationship for a logarithmic plot of these two parameters. The crack propagation results may be analysed by a Paris law of the form:

$$da/dN = C (\Delta J)^n$$

where:

$$C = 1.4151 \cdot 10^{-5}$$

$$n = 1.55$$

#### Toughness measurement

It is important in this type of study to know the level at which tearing begins, a level normally characterised by  $J_{IC}$ .

$J_{IC}$  was determined for the side grooved CT specimens of 35 mm thickness (figure 5); the crack propagation being followed by the electrical potential method.

#### $\Delta J$ CTOD Relationship

A CTOD measurement was performed for different values of "a" (increments of 2 mm). CTOD was measured each time the crack reached the transducer. Another measurement was carried out after the crack tip had passed the transducer (figure 6). Figure 7 shows a typical example (for a given  $\Delta J$  and a given transducer position) of the difference between measured and predicted data.

#### Fractography analysis

Fractographic analysis shows that the crack remains planar due to side grooves.

However the crack front large  $\Delta J$  values is not perfectly linear. There is faster propagation at the edges, due to the concentrations caused by the side grooves but also a slightly faster or slower propagation at the centre which gives a crack front shape as shown in figure 8.

#### Microscopic analysis

Microscopic analysis reveals rough fracture surfaces. The closure and compression cause a flattening of the surfaces particularly when crack propagation takes place at high values of  $\Delta J$ . A new unflattened areas reveal striated zones (figure 9) for low  $\Delta J$  values and dimples, the number of which increases with the  $\Delta J$  level. Although loading was in fatigue, the fracture surfaces resemble surfaces resulting from monotonic loading.

DISCUSSION

Effect of contained yielding

It can be seen that contained yielding is almost demonstrated if constant  $\Delta J$  tests are observed. Examination of the hysteresis curves shows that in parallel with the change in closure effects, the factor  $R = P_{\min} / P_{\max}$  decreases in an acyclic manner. A potential correction formula based on the R ratio is discussed in section 6.

The fact, that the crack propagation rate decreases during constant  $\Delta J$  tests, demonstrates that the method selected for determining  $\Delta J$  from hysteresis loop area will not provide a formal definition of  $\Delta J$ . This is because of the large modification of stress and strain fields produced around the crack tip by closure when the load is released. In practice, however, the variations in  $da/dN$  obtained with constant  $\Delta J$  testing are of the same order of magnitude as the dispersion of values for different specimens.  $\Delta J$  as defined here can be of use for industrial applications, given the accuracy required there.

Propagation rate measurement

The linear relationship between  $\Delta J$  and crack propagation rate demonstrates that the  $\Delta J$  parameter characterizes cracking from the elastic to the plastic range. Cracking can be described by the Paris law (1) using an exponent of 1.55. This is in agreement with results obtained by Kaisand and Mowbray (2), Rye et al (5) and by Dowling (11). Their values were 1.6, 1.5 and 1.56 respectively. Vardar obtained 1.77 for type 1020 steel.

Comparison was performed with the law  $da/dN = f(\Delta J = \Delta K^2/E)$  an extrapolation of the linear fracture mechanics range. These tests were carried out on CT specimens at

$$R = \sigma_{\min} / \sigma_{\max} = 0.1 \text{ for } 20 \text{ MPa } \sqrt{m} < \Delta K < 60 \text{ MPa } \sqrt{m}$$

Effect of thickness

Thickness B in Landes formula is thickness between the side grooves. However, the effective thickness,  $B_{\text{eff}}$ , should be used: The areas of the specimen around the side groove contribute to cracking. The difference in  $\Delta J$  is approximately 10% when the correction given by Devaux et al (16) is used.

$$B_{\text{eff}} = \sqrt{B_{\text{Net}} \cdot B_{\text{tot}}}$$

## FRACTURE CONTROL OF ENGINEERING STRUCTURES – ECF 6

The difference is not significant when represented on a logarithmic scale and it is less than the data scatter (figure 10).

### Toughness measurement

The measured  $J_{Ic}$  is approximately 1500 kN/m. On the  $da/dN$  vs.  $\Delta J$  plot this corresponds to a propagation rate of 1 mm/cycle, a value which was never reached during testing since the measured  $\Delta J$  did not exceed 900 kN/m. The tests demonstrated that formation of the dimples characteristic for tearing under cyclic loads occurs at  $\Delta J$  values below the  $J_{Ic}$  threshold for monotonic loading.

### $\Delta J$ -CTOD Relationship

A knowledge of CTOD provides deformation profiles whatever the  $\Delta J$  and whatever the crack length. Results obtained from CTOD transducers permit a more accurate prediction of the moment of closure when compression begins.

### Influence of R ratio

From the results of crack propagation as a function of  $\Delta J$  (figure 4), it is observed that in the region of extended plasticity (high values of applied  $\Delta J$ ),  $\Delta J$  is a conservative parameter. Even for low values of  $\Delta J$ , the correlation with results on standard specimens shows significant differences. Moreover, in the tests with a constant value of  $\Delta J$ , different crack propagation rates are observed.

All this shows that the correlation of crack propagation rate should not be done with  $\Delta J$  but with another parameter  $(\Delta J)_{eff}$ . In fact, for the tests conducted with  $\Delta J = \text{constant}$  as well as with increasing  $\Delta J$ , the R-ratio is not constant. The literature survey on this subject (cf. (17)) shows that the governing parameter in fatigue crack propagation must take into account the effect of R-ratio. In the case of stainless steels, the following formula was already used:

$$(\Delta J)_{eff} = \Delta J / (1 - R/2)^2$$

In this study, a first attempt is made using this simple formula. Later a fuller study of this effect will be undertaken.

Figure 11 shows that taking into account the effect of ratio R in tests with constant  $\Delta J$ , one obtains different value of  $(\Delta J)_{eff}$ , which could explain the differences observed in crack propagation rates.

## FRACTURE CONTROL OF ENGINEERING STRUCTURES – ECF 6

Moreover figure 12 shows a better representation of experimental results as a function of  $(\Delta J)_{\text{eff}}$  and a better compatibility with results on standard specimens.

### CONCLUSIONS

- \* The correlation between the crack propagation rate (high propagation rates) and the parameter  $\Delta J$  indicates lower growth rates if compared to the classical material data based on  $\Delta K$ .
- \* The crack propagation rate can be correlated with success with the parameter  $(\Delta J)_{\text{eff}}$  which integrates the effect of the R-ratio. In the range of crack propagation rates of  $5 \cdot 10^{-2}$  mm to 0,5 mm/cycle, one obtains a relation of the type:

$$da/dN = C (\Delta J)_{\text{eff}}^n$$

where:

$$C = 3.1 \times 10^{-6}$$

$$n = 2.1$$

- \* The tests at a constant value of  $\Delta J$  but with varying R give different crack propagation rates which confirm the effect of the R-ratio.
- \* The relation between CTOD and  $\Delta J$  permits to know the deformation profile at the edge of the crack whatever the crack position.
- \* During crack propagation at high values of  $\Delta J$ , the formation of dimples appear at J-values lower than  $J_{Ic}$  obtained under monotonic loading tests.

### SYMBOLS USED

A	= area under the load displacement curve
a	= crack length
B	= specimen thickness
b	= remaining ligament
C	= constant in crack growth rate equation
da/dN	= crack growth rate per cycle
$\alpha$	= correction coefficient
n	= exponent in crack growth rate equation

### ACKNOWLEDGEMENTS

The authors thank M. Bhandari, M. Taupin and M. Pellisier-Tanon from Framatome for helpful suggestions.



REFERENCES

- (1) Dowling, N.E., ASTM-STP 637, 1977, pp. 97-121.
- (2) Kaisand, L.R., Mowbray, D.F., ASTM-STP 668, 1979, pp. 270-280.
- (3) Liu, Y.Y., Lin, F.S., Int. Journal of Fatigue, Vol. 6, no.1, January 1984.
- (4) Radhakrishnan, Fat. Eng. Mat. and Struct. Vol. 3, pp. 75-84.
- (5) Rie, K.T., Sohuber, R., Kohler, W., ECF5.
- (6) Landes, J.D., McCabe, D.E., Westinghouse R et D, Scientific paper, pp. 81-107.
- (7) Tomkins, B., Summer, G., Wareing, J., "Proc. Int. Symp. LCF Strength and El. Pl. Behaviour of Mat." Ed.'s Ktaye and E.Haibach, Stuttgart (79) 495.
- (8) Tanaka, Int. Journal of Fracture, 22 (1983), pp. 91-104.
- (9) Wang Shuan Zhu, Yang Sheng, Eng. Fract. Mech.
- (10) Dowling, N.E., Begley, J.A., ASTM-STP 590, 1976, pp. 82-103.
- (11) Dowling, N.E., ASTM-STP 601, 1976, pp. 19-32.
- (12) Clarke, G.A., Landes, J.D., Journal of Testing and Evaluation, Vol. 7, no.5, 1979, pp. 264-269.
- (13) Landes, J.D., Walker, H., Clarke, G.A., ASTM-STP 668, 1979 pp. 266-287.
- (14) Vardar, O., Journal of Eng. Mat. and Technology, Vol. 104, July 1982, pp. 192.
- (15) EPRI, Rapport. An engineering approach for E.P.F.A.
- (16) Devaux et al., 3-D Elastoplastic analysis of 2 CT 50 fracture specimens.
- (17) Bernard, J.L. and Slama, G.S., Nuclear Technology, Vol. 59, 1982.

STAINLESS STEEL Z3CND18-10

C %	Si	Mn	Cr	Ni	Mo	CU
0.028	0.47	1.72	17.48	12.22	2.34	0.21

$R_{e0.2\%}$ MPa	$R_m$ MPa	A %
294	590	56

with  $R_{e0.2}$ : YIELD STRESS  
 $R_m$ : ULTIMATE STRESS  
 A: REDUCTION IN AREA

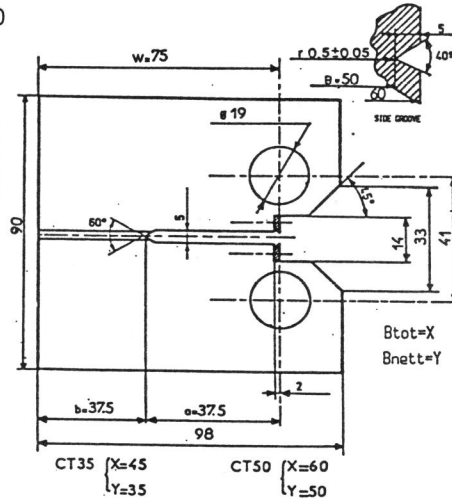


Table 1: Chemical and mechanical properties

Figure 1: Diagram of specimen

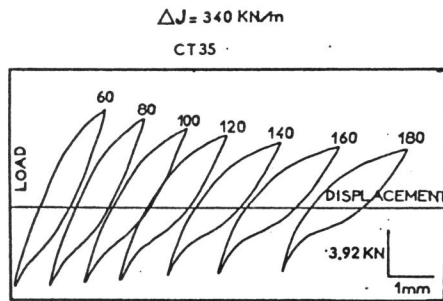


Figure 2: Hysteresis loops with the corresponding cycle numbers

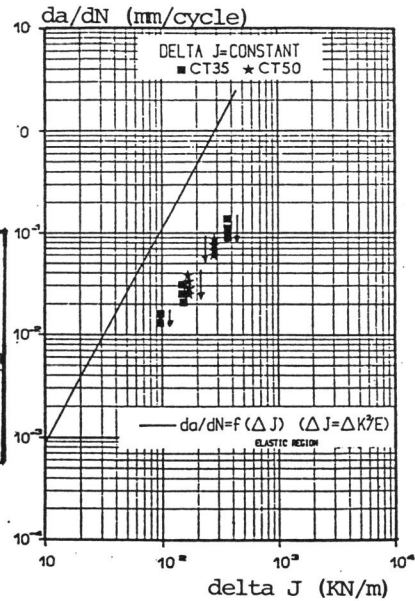


Figure 3:  $da/dN = F$  (constant delta (J))

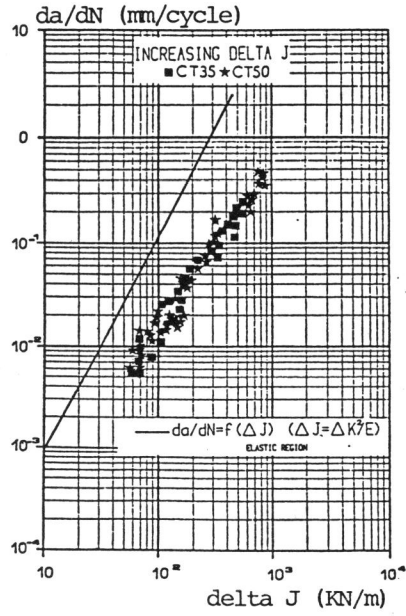


Figure 4:  $da/dN = F$  (increasing  $\Delta J$ )

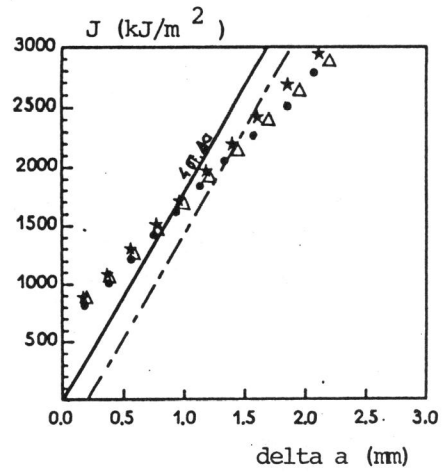


Figure 5: Toughness measurement

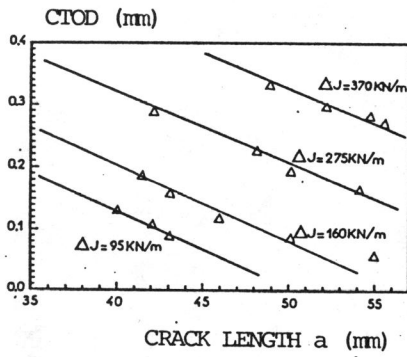


Figure 6: CTOD =  $F(a)$  for given  $\Delta J$

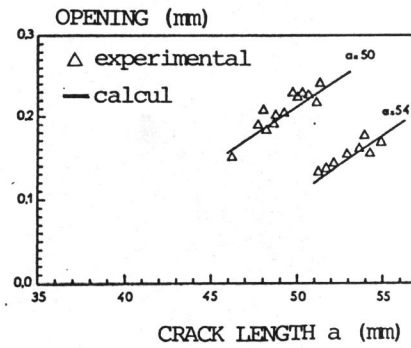


Figure 7: Opening CTOD =  $F(a)$   $\Delta J = 275 \text{ KN/m}$

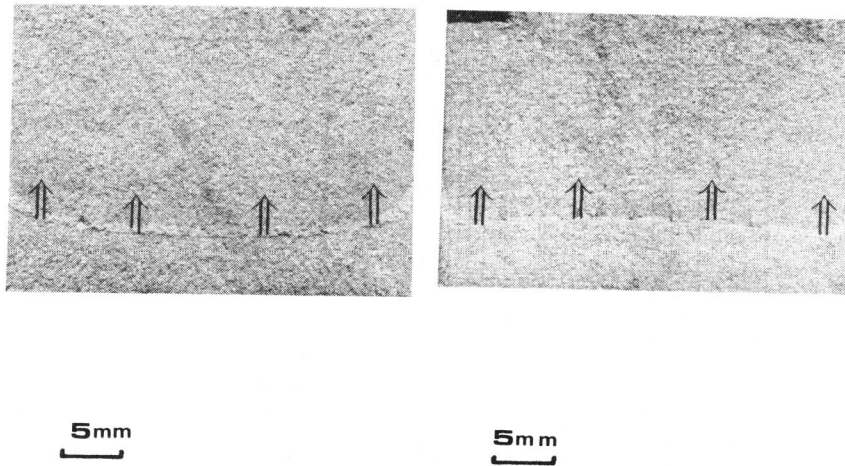


Figure 8: Example of crack front

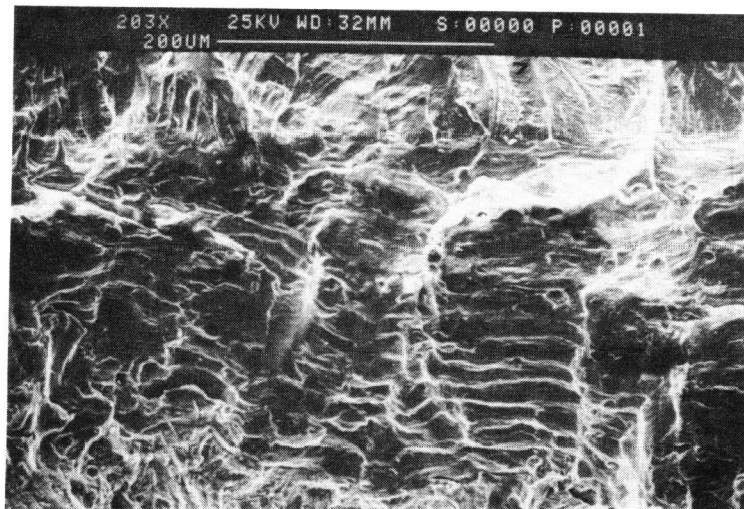


Figure 9: Striated zones for  $\Delta(J) = 200 \text{ kN/m}$

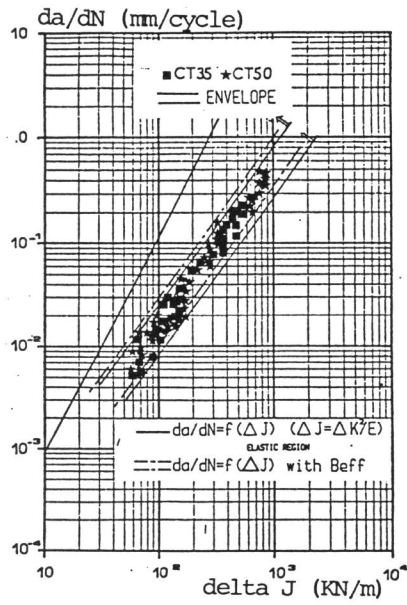


Figure 10: Effect of thickness

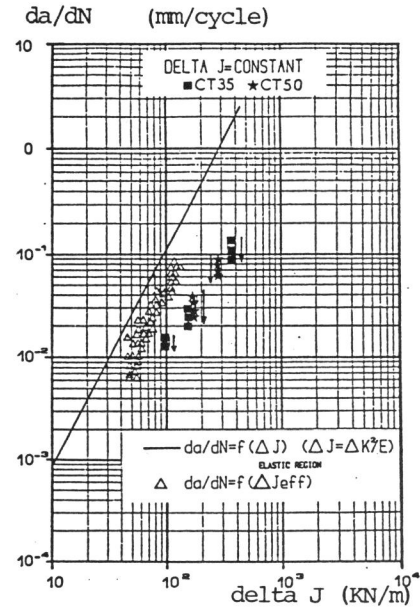


Figure 11:  $da/dN = F(\Delta J_{eff})$

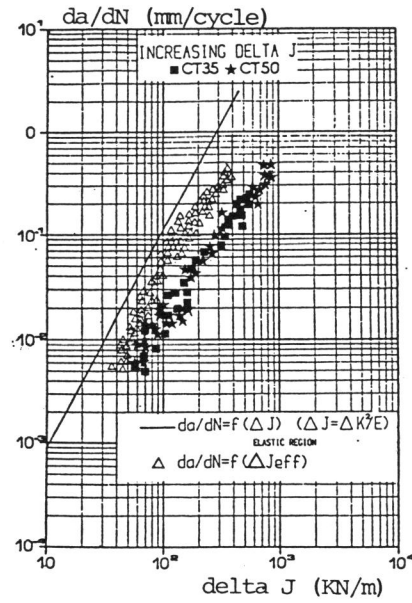


Figure 12:  $da/dN = F(\Delta J_{eff})$